



# Variance of the Flexure Model Predictions With Rejuvenated Volcanism at Kīlauea Point, Kaua‘i, Hawai‘i

**Thor Thordarson<sup>1\*</sup> and Michael O. Garcia<sup>2</sup>**

<sup>1</sup> Faculty and Institute of Earth Sciences, University of Iceland, Reykjavik, Iceland, <sup>2</sup> Department of Geology and Geophysics, University of Hawai‘i at Mānoa, Honolulu, HI, United States

## OPEN ACCESS

### Edited by:

Richard James Brown,  
Durham University, United Kingdom

### Reviewed by:

J. Gregory Shellnutt,  
National Taiwan Normal University,  
Taiwan

Jörn-Frederik Wotzlaw,  
ETH Zürich, Switzerland

### \*Correspondence:

Thor Thordarson  
torvth@hi.is

### Specialty section:

This article was submitted to  
Volcanology,  
a section of the journal  
Frontiers in Earth Science

**Received:** 06 March 2018

**Accepted:** 10 August 2018

**Published:** 04 September 2018

### Citation:

Thordarson T and Garcia MO (2018)  
Variance of the Flexure Model  
Predictions With Rejuvenated  
Volcanism at Kīlauea Point, Kaua‘i,  
Hawai‘i. *Front. Earth Sci.* 6:121.  
doi: 10.3389/feart.2018.00121

The origin of rejuvenated volcanism on mantle plume related oceanic islands remains controversial. One commonly cited model is decompressional melting related to plate flexure from the rapid loading of the lithosphere by the formation of a shield volcano above the plume stem. This model provides testable predictions about the timing and subsidence history of the island. Here we evaluate the flexure model by examining the products of three well dated rejuvenation stage eruptions at Kīlauea Point, Kaua‘i, (Hawai‘i); the  $2.65 \pm 0.35$  Ma Mōkōlea Point lava,  $1.67 \pm 0.11$  Ma for Crater Hill tuff cone and  $0.69 \pm 0.03$  Ma for Kīlauea Point lava events. These eruptions record the flexure of the island over a 2 Ma period, the longest sequence of rejuvenated volcanism within the Hawaiian Islands. These three eruptions, including two subaerial flows (the Mōkōlea Point and Kīlauea Point lavas) and the only phreatomagmatic vent structure on Kaua‘i (the Crater Hill tuff cone), document the progressive sinking and uplift of the island related to sea level as the island drifted away from the Hawaiian hot spot at  $\sim 10$  cm/year. The timing of volcanism and the elevation of Kīlauea Point relative to sea level are inconsistent with the predictions of the flexural melting model. These new results indicate that decompression melting cannot be the sole driver for rejuvenated volcanism on Kaua‘i. Additional explanations are needed to account for the timing and volume of rejuvenated volcanism in Hawai‘i.

**Keywords:** Hawai‘i, Kaua‘i, Kīlauea Point, rejuvenated volcanism, volcanic succession, geochronology, phreatomagmatic, effusive

## INTRODUCTION

Rejuvenated magmatism on Hawaiian and other ocean islands occurs hundreds of kilometers downstream from the stem of the ascending mantle plume following a hiatus of  $\sim 0.5\text{--}2$  millions of years (Myrs) in volcanism (e.g., Macdonald et al., 1983; Garcia et al., 2010). The six oldest of nine main Hawaiian Islands (spanning the age range of  $\sim 6$  to 1.5 Myrs; Garcia et al., 2010) feature rejuvenated volcanism. Although, products of rejuvenated volcanism represent a small fraction of the total volume of individual islands or  $\leq 0.1$  vol. % (e.g., Walker, 1990; Garcia et al., 2010), it poses significant risk on the more densely populated islands (i.e., Kaua‘i, O‘ahu, Moloka‘i, and Maui). The rejuvenated volcanic products are commonly highly alkalic in nature and geochemically distinct from the underlying shield lavas (e.g., Clague and Frey, 1982; Cousens and Clague, 2015).

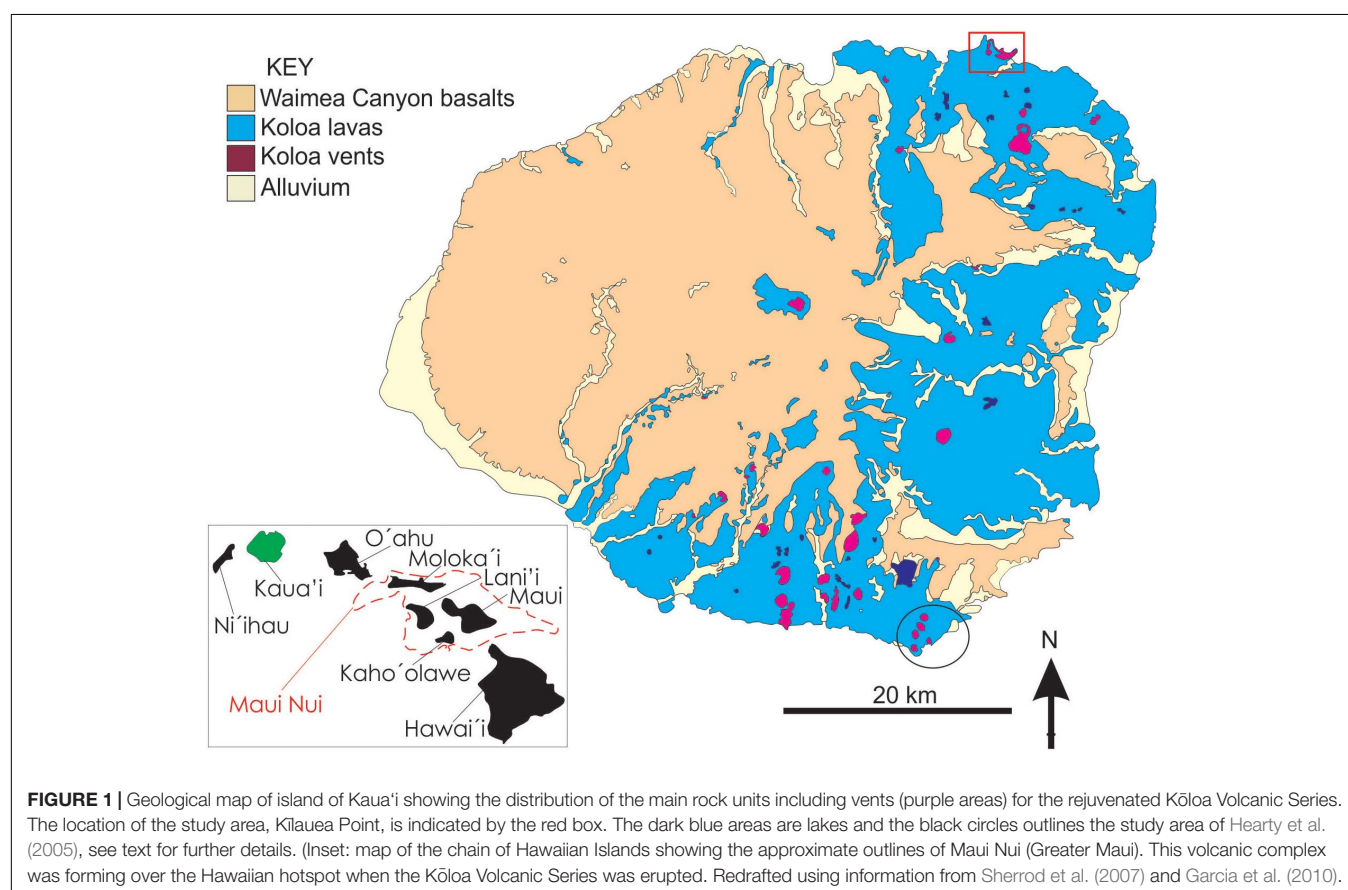
The indication of a depleted source for the rejuvenated magmatism in Hawaii, inferred to be either in the ocean lithosphere or as a component of the deflected mantle plume (e.g., Maaløe et al., 1992; Lassiter et al., 2000; Yang et al., 2003; Fekiacova et al., 2007), has resulted in three conceptual models for its origin: (i) melting of the oceanic lithosphere (e.g., Gurriet, 1987), (ii) decompressional melting of the plume following lateral spreading beneath the lithosphere (e.g., Ribe and Christensen, 1999), and (iii) decompressional melting caused by flexural uplift as a consequence of lithospheric loading above the plume stem (e.g., Jackson and Wright, 1970). Accordingly, as each volcano drifts off the plume, the subsidence is followed by uplift as it rides the fore-bulge of the Hawaiian flexural arch and subsides after passing its crest (e.g., Wessel, 1993). It has been proposed that the distance (i.e., the temporal gap) between the loading islands and the flexural arch is on par with the distance between contemporaneous shield and rejuvenation volcanism, implying that these features are intrinsically linked (e.g., Bianco et al., 2005).

These models provide predictions on the age range of the rejuvenated volcanic constructs as well as the range in erupted magma volumes and compositions. The lithospheric melting and decompressional melting models fail to account for the South and North Arch Volcanic Fields (e.g., Lipman et al., 1989; Clague et al., 1990) that formed on the flexural arch ~250 km off the island-chain axis (e.g., Bianco et al., 2005). However,

the predictableness of the flexural uplift model implies that it could be evaluated, or even validated, via examination of age-constrained sequences of rejuvenated volcanic units. Such an opportunity is provided at Kilauea Point on Kaua'i (**Figure 1**), where three pulses of rejuvenated volcanism span ~2 Myrs, covering the main pulse of rejuvenated volcanism (e.g., Garcia et al., 2010). This site also records two oscillations of the island relative to sea level. Here we present a new map and analysis of the rejuvenated volcanic succession at Kilauea Point. The results and interpretations are used to evaluate the timing of subsidence and flexural uplift, and its impact on rejuvenated volcanism on Kaua'i.

## GEOLOGIC BACKGROUND

The island of Kaua'i features the second oldest and the most voluminous record of rejuvenated volcanism among the Hawaiian Islands, covering the eastern half of the island (**Figure 1**). The rejuvenated lavas rest unconformably on shield-building Waimea Canyon tholeiite lavas (~3.9–5.1 million years ago) and post-shield lava (3.6–3.9 million years ago; Macdonald et al., 1960; Sherrod et al., 2007; Garcia et al., 2010; Cousens and Clague, 2015; Sherrod et al., 2015). The rapid loading of Cretaceous lithosphere under the Hawaiian Islands has caused several km of subsidence for the older shield volcanoes (Moore,



1987). The shield stage shoreline of the island until ~4 million years ago is currently at least 6 km offshore from Kilauea Point and ~0.85 to 1 km below sea level (Flinders et al., 2010). Rejuvenated volcanism on Kaua'i (Kōloa Volcanic Series) formed ~58 km<sup>3</sup> (dense rock equivalent) of alkali basalt tephra cones and lava flow fields between 0.15 and ~2.6 million years ago (Garcia et al., 2010). Recent <sup>40</sup>Ar/<sup>39</sup>Ar dating of chips of basanite and nephelinite from drilling in Lihue Basin reveal ages in the range of ~3.1 to ~3.4 million years ago (e.g., Sherrod et al., 2015), suggesting that Kōloa-like magmatism may have followed the post-shield stage without a significant break in volcanic activity (e.g., Cousens and Clague, 2015). About 40 widely dispersed Kōloa vent structures have been identified (Macdonald et al., 1960). Most of the vent structures consist of scoria or spatter cones and their associated 'a'a and pāhoehoe lava flow fields cover the lowlands the eastern side of the island and also filled many of the deep valleys on the island to depths of hundreds of meters (Macdonald et al., 1960; Garcia et al., 2010). Volcanic units within the Kōloa Volcanic Series are either separated by sedimentary deposits (mostly conglomerates) or soil horizons. The northernmost subaerial Kōloa vents are found at Kilauea Point on the northeast shore of the island (Figure 1). Here the volcanic succession is unique in the Hawaiian Islands in recording at a single location three eruptive events spanning the bulk of the main period of rejuvenation stage volcanism on Kaua'i as well as preserving the only phreatomagmatic vent structures of the Kōloa Volcanic Series (Macdonald et al., 1960).

## VOLCANIC SUCCESSION AT KĪLAUEA POINT: LITHOLOGY, ARCHITECTURE AND HISTORY

Our new geological map of the Kilauea Point area highlights the superbly exposed Kōloa volcanic sequence (Figure 2). Here a nephelinite lava outcrops at the nearby Mōkōlea Point. It is overlain by a ~90-m-thick cone sequence of phreatomagmatic tephra, which is cut by ~1-m-thick olivine-bearing basanitoid dike that produced a ~100-m-thick fountain-fed basanite spatter and lava that cap the succession (Figures 2, 3a). These three eruptive units are referred to here, from the oldest to the youngest, as the Mōkōlea Point lava, Crater Hill tuff cone, and Kilauea Point lava.

### Mōkōlea Point Lava (2.65 Ma)

The Mōkōlea Point lava is exposed along the base of the Mōkōlea Point (Figures 2, 3). The Mōkōlea Point lava is ≥8 m thick at the northern tip of the point as its lower contact is submerged (Figure 3). The upper part of this exposure consists of decimeter to meter thick pāhoehoe sheet lobes and spongy pāhoehoe (i.e., equivalent to P- and S-type pāhoehoe of Wilmoth and Walker, 1993). Figure 4 illustrates the typical three-fold vertical division of the Mōkōlea Point lava lobes into vesicular upper crust, lava core and basal crust, which is indicative of emplacement by insulated transport and flow inflation (e.g., Self et al., 1998; Thordarson and Self, 1998). On the northern tip of the Mōkōlea Point and at the very top of the lobe sequence,

a 0.5–2 m-thick sheet lobe is separated from the rest of the Mōkōlea Point lava by 5–20 cm-thick normally graded, ash to fine lapilli tephra bed (Figure 3d). The tephra contains abundant sub-mm size olivine macrocrysts, similar to those observed in the Mōkōlea Point lava. Also, morphologically and petrographically the top lobe is identical to the lobes beneath the tephra. This indicates that a distinct explosive phase with associated tephra fallout that took place toward the end of the Mōkōlea Point eruption. Consequently, the top lobe represents a late-stage lava emplacement in that event.

The pāhoehoe nature of the Mōkōlea Point lava confirms that it was formed by a subaerial eruption. The surface of the lava slopes inland (i.e., to the west-southwest, Figures 2, 3b) at a shallow angle of ~1°. It drops 8 m over a distance of 620 m disappearing below sea level to the west along the shoreline of the bay (Figure 2). It is noteworthy that upper surface of the Mōkōlea Point lava is partly eroded, providing evidence of subaerial erosion. The distinctive slope of the flow surface strongly indicates that the lava advanced from the east-northeast, implying that the source vent was located ocean ward of the present-day shoreline (Figure 5). Hence, when the Mōkōlea Point lava formed at ~2.6 Ma, the island of Kaua'i stood significantly higher relative to sea level than it does at present.

Sample KR-5 (Table 1) was collected from a quarry on the east side of the point from a weakly vesicular (<0.5 vol. %) pāhoehoe sheet lobe (X on MP-lava in Figure 2). It is an olivine and melilite phryic nephelinite (foidite; Figure 6A) with 10–15 vol. % olivine (>0.5 mm) and 15–25 vol. % melilite microphenocrysts (0.1–0.5 mm) along with rare cm-size dunite fragments (Figure 3c) in a fine-grained (<0.1 mm) holocrystalline matrix dominated by clinopyroxene with lesser nepheline and magnetite plus minor melilite. No secondary minerals were observed. An unspiked K-Ar age determination on the groundmass from this sample gave an eruption age of 2.65 ± 0.35 Ma (Table 1), making it the oldest verified Kōloa event on Kaua'i. It is also one of the most alkalic lavas on Kaua'i, probably produced by very low degree of partial melting (Figure 6B).

### Crater Hill Tuff Cone (1.67 Ma)

The Crater Hill tuff cone is the only known Kōloa phreatomagmatic vent (e.g., Macdonald et al., 1960). The 2-km-long coastal cliff exposure from Mōkōlea Point to Kilauea Point (Figure 2) is comprised of >90 m-thick, bedded phreatomagmatic tephra sequence (Figure 7). This sequence is a remnant of ~2-km wide tuff cone, which is twice the size of the famous Honolulu landmark Diamond Head and larger than any other Hawaiian tuff cone. It is comprised of a well-bedded sequence with a radial dip of 11–21° (Figure 2). The intercepts of dip-directions (Figure 5) indicate a probable vent location about 750 m off the shore. The base of the tuff cone is exposed at Mōkōlea Point, where the tephra sequence rests on the Mōkōlea Point lava.

The lowest part of the tuff cone consists of three meters-thick, very poorly sorted, massive lapilli-tuff breccia (LTB) units featuring decimeter to a meter-size ballistic blocks and juvenile bombs often forming similarly large bomb-sags. The LTB units are intercalated with decimeter-thick units of cross-bedded and

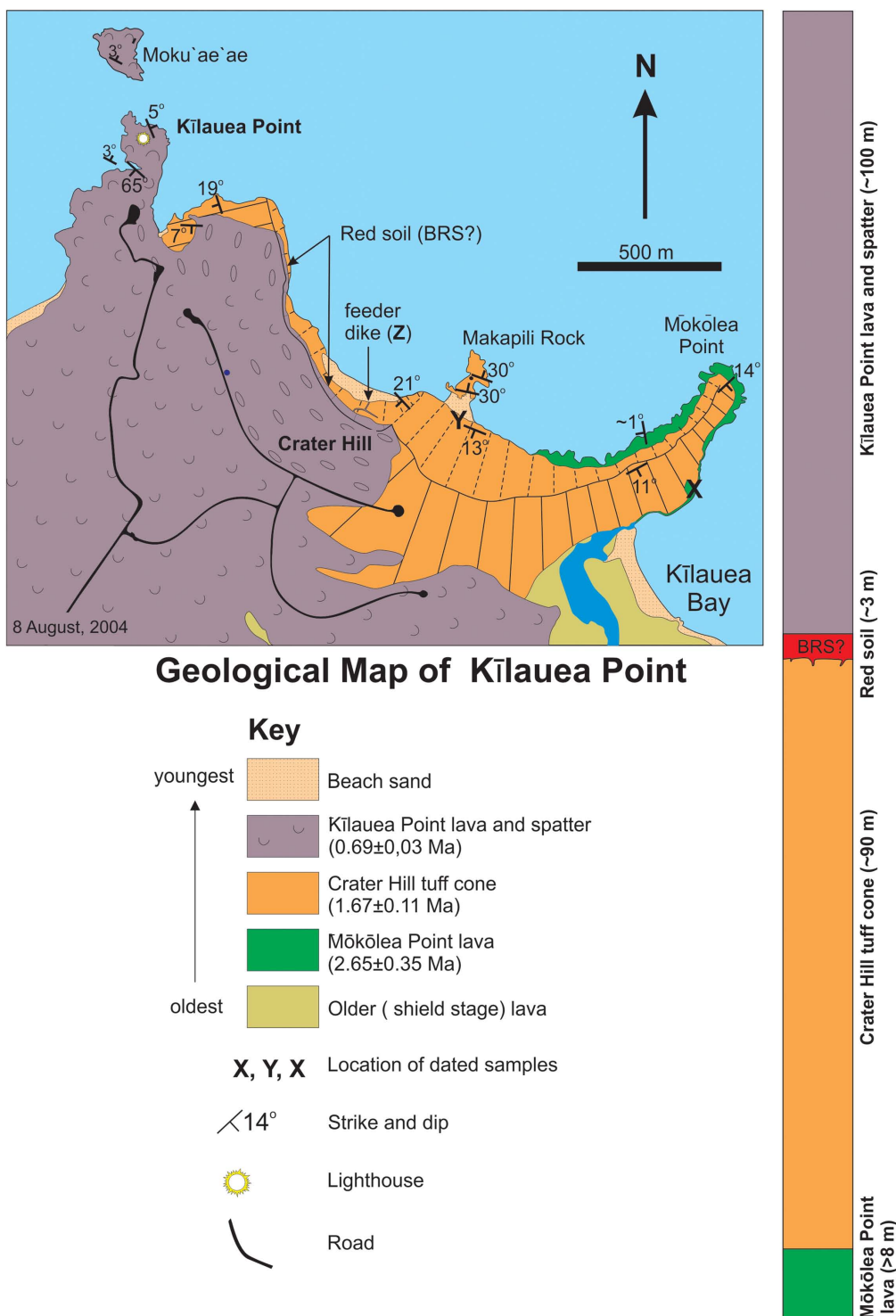


**FIGURE 2 |** Geological map and simplified stratigraphic column (right) of the Kōloa Volcanic Series at Kīlauea Point, Kaua'i based on new mapping. The red soil horizon is not visible on the map, but its position is indicated as shown on the stratigraphic column. BRS stands for the Big Red Soil. See text for further details.

ash-rich lapilli tuff (LT1 on **Figure 7**). The upper part of the sequence of the tuff cone consists of alternating decimeter to a few meters thick lapilli tuff (LT2) and tuff (T) units (**Figure 7**). The LT

units are diffuse-bedded, poorly sorted lapilli tuffs with multiple meters-long, clast-supported pumice lapilli lenses (**Figure 7**). The bedding is frequently deformed by decimeter-size ballistic blocks

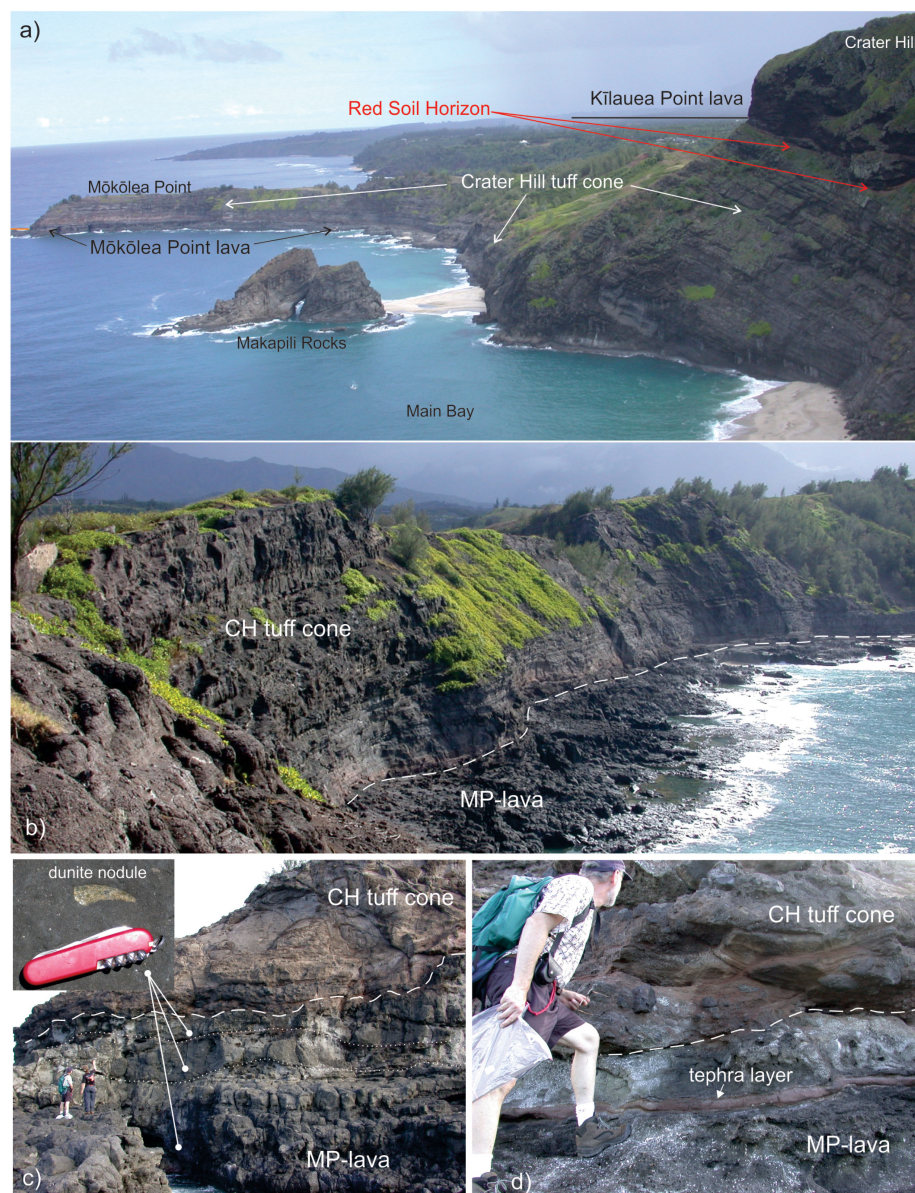
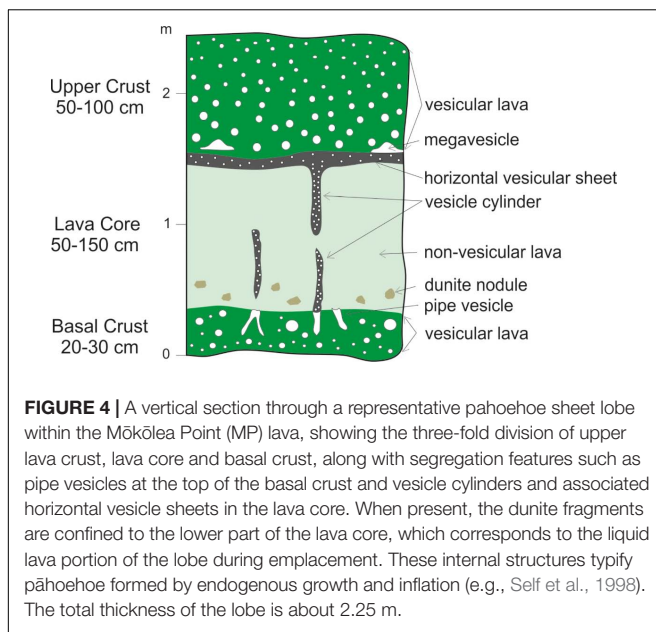


**FIGURE 3 |** Photographs of the Kilauea Point area. **(a)** Oblique view looking east along the coast from Kilauea Point. **(b)** The Mōkōlea Point (MP) lava and lowest part of the Crater Hill (CH) tuff cone sequence at Mōkōlea Point. View looking south from the north end of the point illustrating the slight southward dip of the MP lava surface (indicated by white broken line). **(c)** A stack of three, decimeters to meters thick, pahoehoe sheet lobes overlain by the CH tuff cone deposits (white broken line) at the northern tip of the point. View is to the east. The thickest sheet lobe is at the base and the thinnest at the top (the white dotted lines indicate lobe boundaries). Each lobes contains dunite nodules (inset) in its lava core, as indicated by the circle-ended bars. The boundary between the top two lobes is demarcated by a cm-thick alkali basalt tephra fall deposit (see d for close up). The overlying CH tuff cone deposits consist of massive lapilli-tuff breccia (LTB) units. People (lower left) for scale. **(d)** Close up of the contact (white broken line) between the MP-lava and the CH tuff cone. The white arrow points to the tephra layer that separates the top two lobes of the MP-lava. View is to the east.

and bombs. The T units are either comprised of cross-bedded, moderately sorted medium to coarse ash (T1 on **Figure 7**) or diffuse cross- or planar-bedded, very poorly sorted ash with dispersed armored and accretionary lapilli (T2 on **Figure 7**).

We interpret the LBT units to have been formed by discrete tephra jets fed by rooster-tail explosions at the onset of the eruption. The diffuse-bedded and poorly sorted LT units are

taken to represent aggradational deposition from simultaneous fall and flow sustained but pulsating activity lasting for several hours. Such activity has also been described as continuous uprush (Thorarinsson, 1967). The lapilli fraction corresponds to the tephra fall, while the ash-grade portion is deposited by dilute pyroclastic density currents (i.e., base surges). The cross- and planar-bedded tuffs are interpreted to have been



emplaced by dry (T1) and wet (T2) dilute pyroclastic density currents (**Figure 7**). Their occurrence as distinct horizons in-between the LT units indicates that they were formed after a brief lull in the activity. By analog to the 1963–1967 Surtsey eruption in Iceland, the early stage rooster tail explosions were formed

when the crater was inundated by sea water, while the periods of continuous up-rush took place when the crater alternates from being almost free of and partly filled with sea water (Thorarinsson, 1967). These evidence, along with the presence of reef-limestone fragments in Crater Hill deposits, are consistent with the interpretation that the eruption site was in shallow coastal waters. Thus, when the Crater Hill tuff cone was formed at  $\sim 1.7$  Ma sea level relative to the island was almost the same as today.

A juvenile bomb (KR-2 in **Table 1**) collected from the tuff cone (labeled Y on **Figure 2**) is a weakly vesicular (<5 vol. %) olivine nephelinite (foideite **Figure 6A**) with 5–8 vol. % olivine and minor (1–2 vol. %) of 0.1–0.5 mm clinopyroxene microphenocrysts sitting in a holocrystalline matrix of clinopyroxene, nepheline and magnetite. Some olivine have thin (<0.01 mm thick) rims of iddingsite but no other secondary minerals are present. An unspiked K-Ar age determination on the groundmass of this bomb gave an eruption age of  $1.67 \pm 0.11$  Ma (**Table 1**).

## The Red Paleosol Horizon

The Crater Hill tuff cone sequence and Kilauea Point lava are separated by a 2–3 m thick red paleosol (i.e., saprolite) horizon formed by weathering of the tuff cone tephra during sustained surface exposure (**Figures 3a, 7**). It signifies that a substantial weathering period between eruptions consistent with the  $\sim 1$  Myr age difference between the Crater Hill tuff cone and the Kilauea Point lava (i.e., **Table 1**). This paleosol horizon is probably

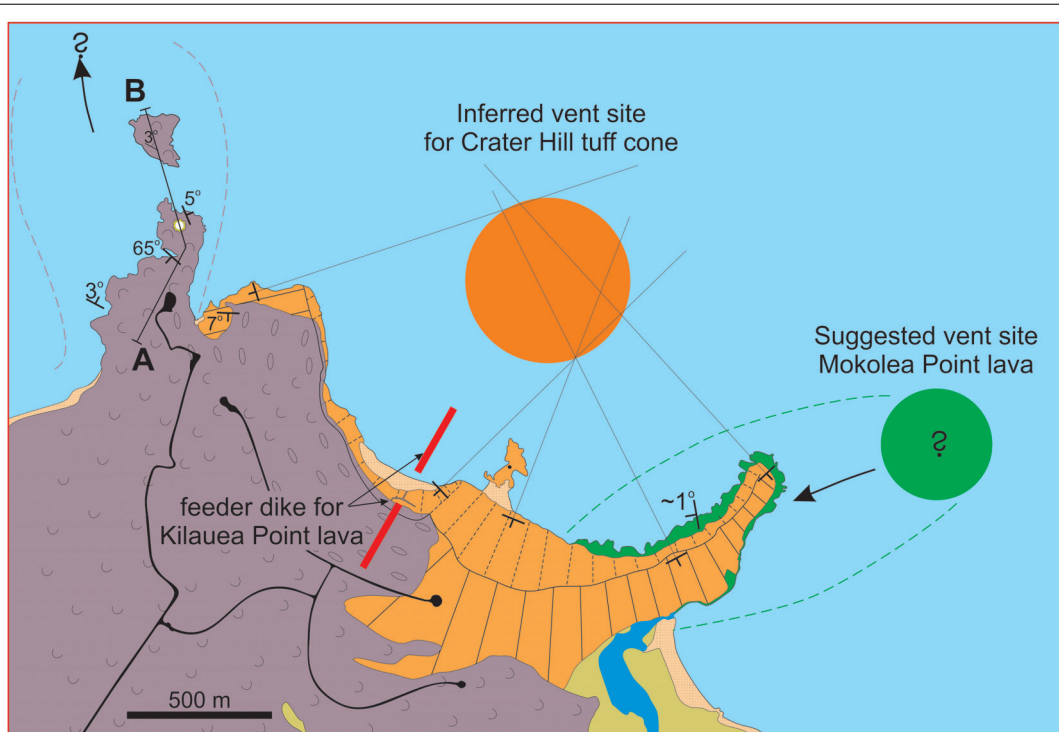


**FIGURE 5 |** Proposed vent positions for the Kilauea Point eruptions. The circles show the inferred vent positions of Mōkōlea Point lava (green) and Crater Hill tuff cone (orange). The broken red line marks the inferred position of the Kilauea Point lava feeder dyke. The Line A-B indicates the location of the cross section in **Figure 7**. The strike and dip symbols for bedding in the tuff cone are shown without dip values for sake of clarity (see **Figure 2** for values).

**TABLE 1 |** The rock type, chemical composition and unspiked K-Ar ages for the three Kōloa Volcanic Series units making up the succession at Kīlauea Point on the island of Kaua'i.

Sample	Mōkōlea Point lava (KR-5)	Crater Hill tuff cone (KR-2)	Kīlauea Point lava (KR-3)
Rock type	Olivine-melilite nephelinite	Olivine nephelinite	Basanite
<b>Major elements (wt.%)</b>			
SiO <sub>2</sub>	37.75	39.90	43.53
TiO <sub>2</sub>	3.46	3.31	2.81
Al <sub>2</sub> O <sub>3</sub>	9.25	10.14	13.55
Fe <sub>2</sub> O <sub>3</sub> *	15.39	14.44	13.40
MnO	0.23	0.21	0.19
MgO	14.42	13.67	6.88
CaO	13.29	12.75	14.39
Na <sub>2</sub> O	3.32	3.61	2.67
K <sub>2</sub> O	0.98	0.49	1.30
P <sub>2</sub> O <sub>5</sub>	0.93	0.70	0.49
Total	99.01	99.21	99.20
<b>Trace elements (ppm)</b>			
V	323	270	310
Cr	493	528	336
Ni	329	331	111
Rb	27	10	30
Sr	1085	802	699
Y	25	22	21
Zr	292	203	151
Nb	88	69	51
Ba	991	763	708
La	59	46	30
Ce	127	98	59
Age (Ma)	2.65	1.67	0.69
1 sigma	0.35	0.11	0.03

For further information on samples and analytical procedures see Garcia et al. (2010). The labels given in the parenthesis are sample numbers. \*Total iron as Fe<sub>2</sub>O<sub>3</sub>.

the time equivalent of the Big Red Soil (BRS) of Hearty et al. (2005) on the south coast of Kaua'i. The BRS is 0.5–1.5 m thick and present within a raised carbonate platform formation. It is thought to have formed during a prolonged surface exposure of the platform between 0.5 and 1.0 Ma (Hearty et al., 2005).

## Kīlauea Point Lava (0.69 Ma)

The Kīlauea Point lava is the youngest eruptive unit at Kīlauea Point. The north to south trending dike connects to the Kīlauea Point lava near the center of coastal outcrop (Figures 2, 6). The near-vent deposits are ~100-m-thick accumulation of spatter and scoria, representing a crater rampart that rests directly on the red paleosol horizon at the top of Crater Hill tuff cone sequence (Figure 7). Down slope, this succession grades into >60-m-thick fountain-fed lava flow that was flowed south and northwest from the erupting fissure (Figure 2). The lava features a massive columnar jointed core that is flanked by compound pāhoehoe lobes (Figure 8). The massive facies may represent the fill of lava channel and the compound facies probably were levees

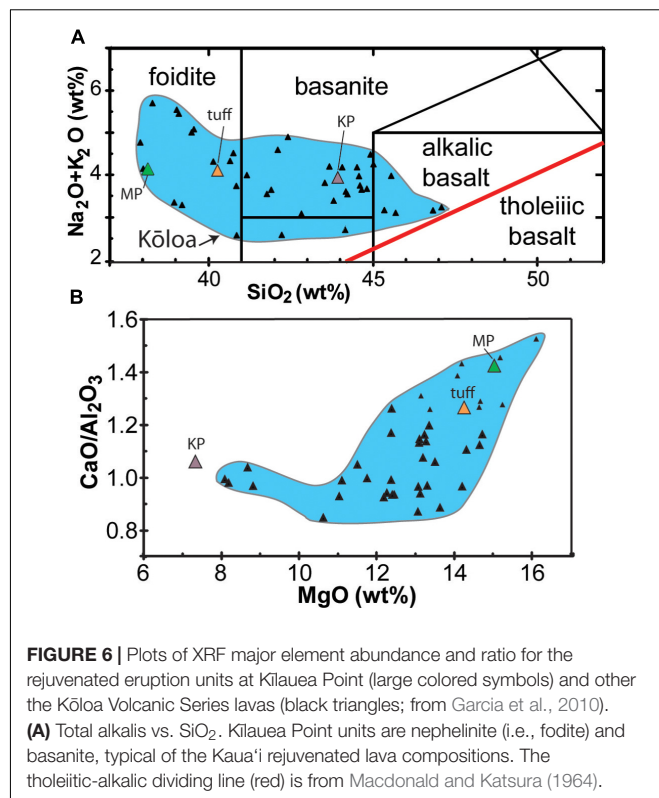


**FIGURE 6 |** Plots of XRF major element abundance and ratio for the rejuvenated eruption units at Kīlauea Point (large colored symbols) and other the Kōloa Volcanic Series lavas (black triangles; from Garcia et al., 2010). **(A)** Total alkalis vs. SiO<sub>2</sub>. Kīlauea Point units are nephelinite (i.e., foidite) and basanite, typical of the Kaua'i rejuvenated lava compositions. The tholeiitic-alkalic dividing line (red) is from Macdonald and Katsura (1964). **(B)** CaO/Al<sub>2</sub>O<sub>3</sub> vs. MgO. Kōloa Volcanics. The higher CaO/Al<sub>2</sub>O<sub>3</sub> value is indicative of larger degree of partial melting and the horizontal offset removal of olivine by fractional crystallization. MP: Mōkōlea Point lava, tuff: Crater Hill tuff cone, KP: Kīlauea Point lava.

and overbank flows. The northwest branch of the Kīlauea Point lava extends seaward at least to the islet of Moku'ae'ae (>300 m beyond the present coastline; Figure 2). A 3° dip of lobe contacts and laterally continuous internal planes indicate that the flow may extend >20–30 m below sea level at Moku'ae'ae (Figure 8). Therefore, the Kīlauea Point lava must have been emplaced when sea level relative to the island stood was 10's of meters lower than today.

Sample KR-3 is from Kīlauea Point lava feeder dyke which yields an unspiked K-Ar eruption age of  $0.69 \pm 0.03$  Ma (Table 1). It is comprised of nearly aphyric basanite (Figure 4a) with <1 vol. % olivine phenocrysts and microphenocrysts of clinopyroxene (3–5 vol. %) in a holocrystalline matrix of clinopyroxene, nepheline and magnetite (no plagioclase). It is massive and moderately vesicular (15–25 vol. %) with calcite partially filling some vesicles.

## DISCUSSION

### Vertical Movement of the Island of Kaua'i Revealed by the Kōloa Succession at Kīlauea Point

The rapidly loading of the ~90 million year old Pacific Ocean lithosphere by a growing Hawaiian volcano causes the crust to

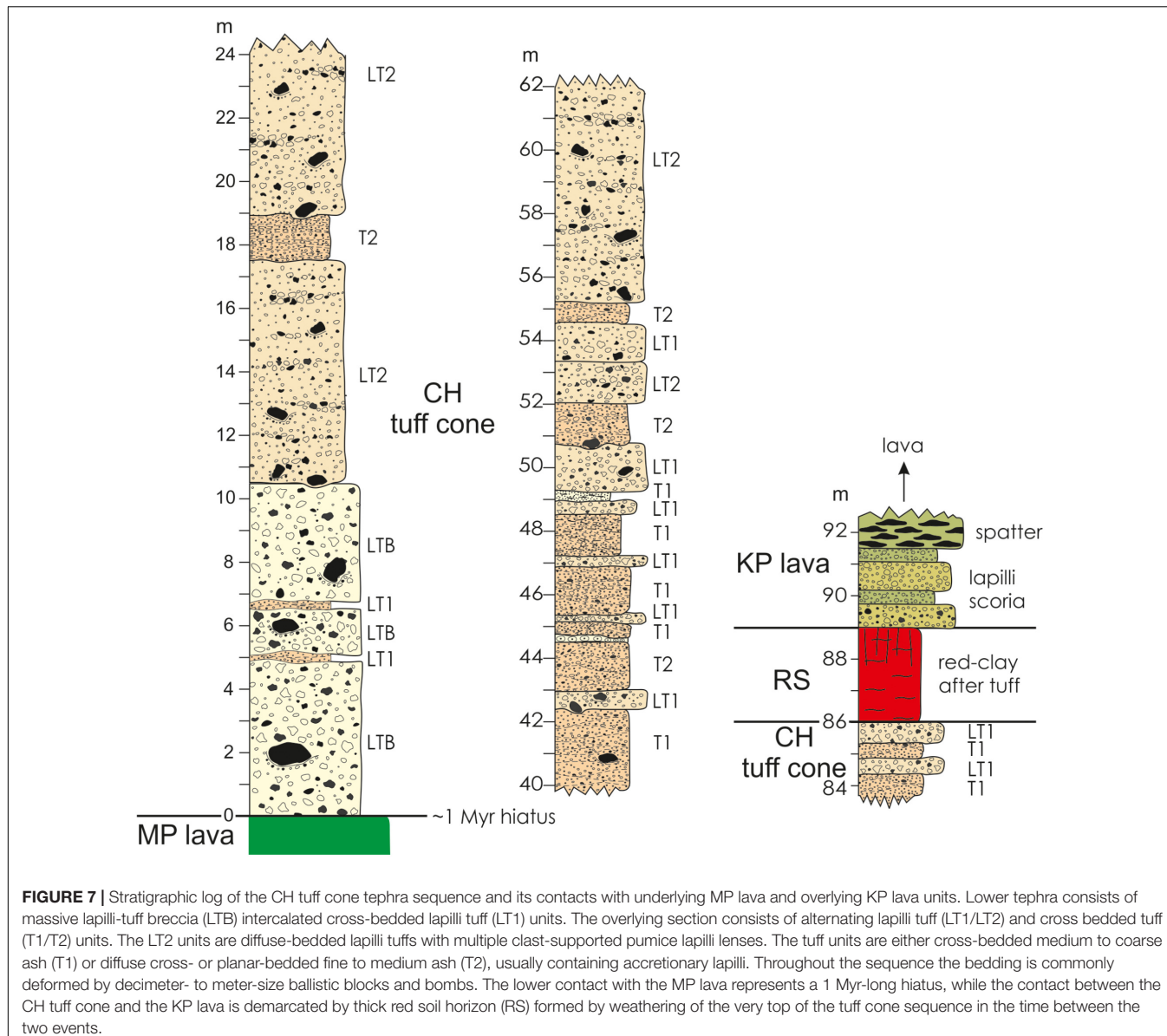


**FIGURE 7 |** Stratigraphic log of the CH tuff cone tephra sequence and its contacts with underlying MP lava and overlying KP lava units. Lower tephra consists of massive lapilli-tuff breccia (LTB) intercalated cross-bedded lapilli tuff (LT1) units. The overlying section consists of alternating lapilli tuff (LT1/LT2) and cross bedded tuff (T1/T2) units. The LT2 units are diffuse-bedded lapilli tuffs with multiple clast-supported pumice lapilli lenses. The tuff units are either cross-bedded medium to coarse ash (T1) or diffuse cross- or planar-bedded fine to medium ash (T2), usually containing accretionary lapilli. Throughout the sequence the bedding is commonly deformed by decimeter- to meter-size ballistic blocks and bombs. The lower contact with the MP lava represents a 1 Myr-long hiatus, while the contact between the CH tuff cone and the KP lava is demarcated by thick red soil horizon (RS) formed by weathering of the very top of the tuff cone sequence in the time between the two events.

subside at rate of  $\sim 2.6$  mm/year (Moore, 1987; Ludwig et al., 1991). As each volcano drifts off the plume, the subsidence is followed by uplift as it rides up the Hawaiian flexural arch and subsides again after passing its crest (e.g., Wessel, 1993). The island Kaua'i has been exposed to this type of “subsidence-rise-subsidence,” with a vertical extent of  $\sim 500$  m or more, during the 5 Myr passage from its formation above the Hawaiian mantle plume to its current position. It has been hypothesized that the distance (=the temporal gap) between the loading islands and the flexural arch is similar to the distance between contemporaneous shield and rejuvenation volcanism, underpinning the proposal that these features are intrinsically linked (e.g., Bianco et al., 2005).

The succession of Kōloa volcanics at Kilauea Point is unique in the Hawaiian Islands in that it provides, at one location, three rejuvenated eruptive units spanning  $\sim 2$  Myrs all recording

formation at different sea level stands (Figure 9). Furthermore, it is evident, that at the time of the Crater Hill eruption ( $\sim 1.7$  Ma) the relative sea level was similar to the present, while the overlying  $\sim 0.7$  Ma Kilauea Point lava and underlying  $\sim 2.7$  Ma Mōkōlea Point lava were formed when the relative sea level was substantially lower than today (Figure 9). Thus, the volcanic succession at Kilauea Point records a subsidence of the island of Kaua'i in the  $\sim 1$ -Myr-long hiatus between the formation of Mōkōlea Point lava and the Crater Hill tuff cone and a rise at least up until formation of the Kilauea Point lava, again followed subsidence (Figures 9, 10).

Kilauea Point is situated about 1000 m above paleoshoreline of Kaua'i near the end of its shield-building stage (Flinders et al., 2010). It follows for Crater Hill tuff cone eruption to have taken place at sea level at  $\sim 1.7$  Ma, the island of the Kaua'i subsided  $\sim 1000$  m in the time between drifting off the hot spot at  $\sim 3.9$  Ma

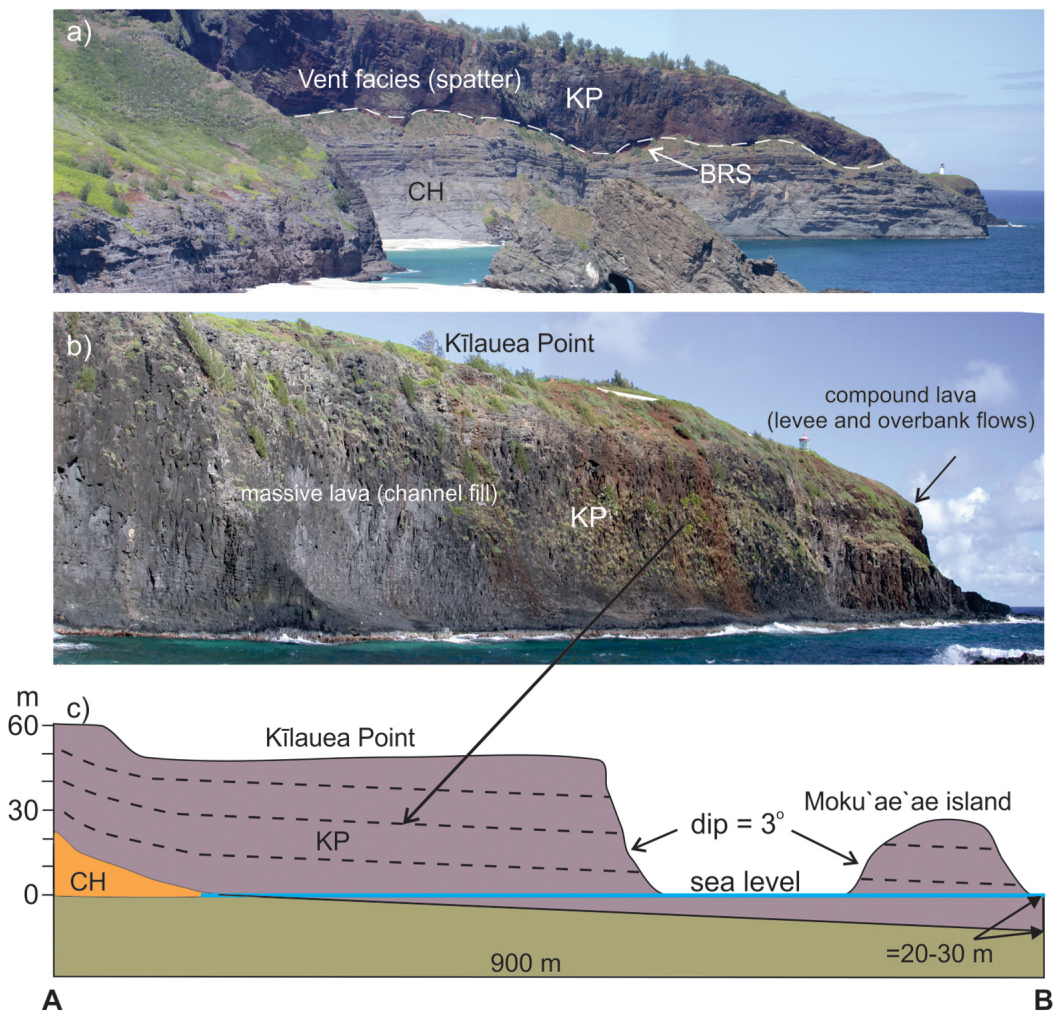


**FIGURE 8 | (a)** The vent facies of the Kilauea Point (KP) lava on top of the Crater Hill (CH) tuff cone at the main bay. The view is to the west. The white broken line delineates its contact between the two eruptive units. Directly below the contact is a 2–3 m-thick red soil horizon (BRS). **(b)** The massive KP lava (channel fill) facies at Kilauea Point flanked by the compound lava. View is to the northwest. **(c)** Schematic cross section of the KP lava from Kilauea Point to Moku`ae`ae island (see Figure 2 for position) illustrating the seaward dip of the strata and the minimum degree of subsidence since formation (lower right).

and the Crater Hill eruption. This indicates a mean subsidence rate of 0.45 mm/year for this period. This rate is about a factor six lower than the current subsidence rate of the Big Island of Hawaii, which is ~2.6 mm/year over the last 0.46 Myrs (Ludwig et al., 1991). However, the estimated average subsidence rate of O'ahu since its shield volcanoes became inactive at ~2.2 Ma (Yamasaki et al., 2011) was also slow (~0.3 mm/year, equal to 600 m of subsidence; Walker, 1990), because it has been counterbalanced by an uplift rate in the range of 0.015–0.06 mm/year (equal to 7.5–30 m of uplift) over the last 0.5 Myrs (Hearty, 2002; McMurtry et al., 2010). Moore (1987) indicated the subsidence rate of the Hawaiian Islands is highest during the first million years. Volcano subsidence rate decreases from 2.6 mm/year to <0.3 mm/year as it migrates away from the mantle plume. Using the mean subsidence rate of 0.45 mm/year for Kaua'i in the period ~3.9 to ~1.7 Ma implies that the Kilauea Point area would have been situated 500–600 m above sea level at the time of the Mōkōlea

Point lava eruption at ~2.7 Ma. These vertical movements on the scales of 100's of meters make it unlikely that the cyclic changes in the relative sea level described above are recording the rise and fall of the global sea level during the latter stages of the Plio-Pleistocene period, because in non-glaciated areas those changes have amplitudes of meters to 10's of meters (e.g., Hearty et al., 2005; Hansen et al., 2013). Our data do not allow assessment of the islands' rise rate during the period between the ~1.7 million year old Crater Hill tuff cone and the ~0.7 million year old Kilauea Point lava eruption. The rise rate of Kaua'i as it ascended the Hawaiian flexural arch was probably similar to the rate estimated for nearby O'ahu, or  $\geq 0.015\text{--}0.06 \text{ mm/year}$  (Hearty, 2002; McMurtry et al., 2010). This implies a rise of 15–60 m for the island in the period leading to the Kilauea Point lava eruption. Hearty et al. (2005) describe three older couplets (I–III) that are separated from the younger ones by the Big Red Soil (BRS) that was developed during the period

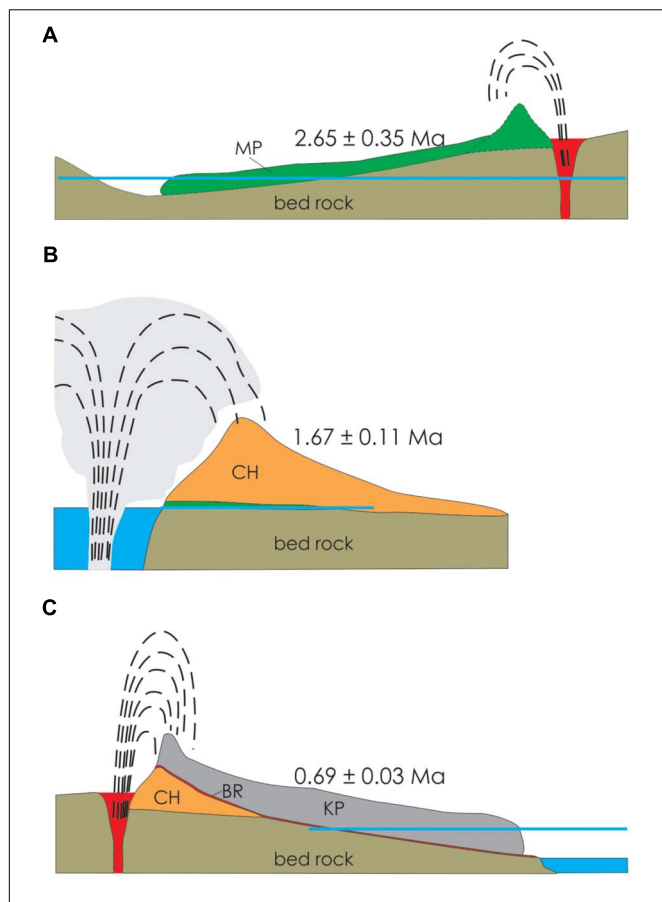


**FIGURE 9 |** Schematic illustrations of the three eruption scenarios from a viewpoint looking west: **(A)** Mōkōlea Point lava (MP), **(B)** Crater Hill (CH) and **(C)** Kilauea Point lava (KP) events. BR indicates the red soil horizon (see text for details). Age of each event is indicated and the blue horizontal line indicates current sea level. Sea level at the time of the eruptions is shown by the blue pattern. Note the illustrations are not drawn to scale and the presence of a cone in **(A)** is inferred.

from ~1.0 to ~0.5 Ma by sustained upward tectonic motion of the island of Kaua'i as it crossed the fore-bulge of the Hawaiian flexural arch, a passage expected to have taken about 0.9 Myrs. The red paleosol horizon at top of the Crater Hill tuff cone sequence developed during approximately the same time interval, i.e., from ~1.7 and ~0.7 Ma, underpinning the inferences made by Hearty et al. (2005). Hence, we conclude that the volcanic succession at Kilauea Point records the key vertical tectonic movements (i.e., “subsidence-rise-subsequence”) during the last ~3 Myrs when the island of Kaua'i traveled from the hot spot over and down the Hawaiian flexural arch to its current location (**Figure 10**).

## The Kilauea Point Succession and the Rejuvenated Volcanism-Flexural Decompression Model

Here we evaluate how the scenario outlined above conforms to the rejuvenated volcanism-flexural decompression model of Bianco et al. (2005). In addition to the observations on

Kaua'i presented above, it is useful to consider these additional observations:

- The paleo-island Maui Nui (**Figure 1**, inset), which consisted of seven shield volcanoes, provided the crustal loading when Kaua'i was passing over the flexural moat and arch. Kaua'i is situated about 350 km west-northwest of the weighted center of Maui Nui (represented by West Maui), about 250 km from western Maui Nui (=West Moloka'i) and 370 km from eastern Maui Nui (=Haleakalā). The Maui Nui volcanoes featured its major shield-building phases in the period from > 2.1 to 0.95 Ma (e.g., Sinton et al., 2017).
- Current distance from the volcanoes producing the crustal loading (i.e., the Island of Hawai'i volcanoes) to the flexural moat is in the range of 110–140 km and about 250 km to the crest of the flexural arch. For the purpose of this discussion, similar distance values are assumed for the times of Maui Nui.
- Assuming a plate spreading rate of 10 cm per year (e.g., Garcia et al., 1987), the island of Kaua'i had been displaced from the anticipated loading shield volcanoes at the time of the ~2.7 Ma Mōkōlea Point lava, the ~1.7 Ma Crater Hill tuff cone and the ~0.7 Ma Kilauea Point lava eruptions as indicated in **Figure 10**.
- Rejuvenated volcanism on Kaua'i spans at least 2.45 Myrs (2.65–0.15 Ma; Garcia et al., 2010) and possibly 3.25 Myrs (3.4–0.15 Ma; e.g., Cousens and Clague, 2015).
- About 58 km<sup>3</sup> magma was erupted during Kaua'i's rejuvenation stage (Garcia et al., 2010). The reconstructed magma production rate indicates steady increase in magma production from onset of rejuvenated activity at ~2.65 to ~1.3 Ma, followed by a sharp decline until ~0.8 Ma and stops at 0.15 Ma (**Figure 10**).

The data presented in this paper along with the evidence collated above on the Kōloa Volcanic Series highlight significant inconsistencies between the flexural decompression model as outlined by Bianco et al. (2005) and data obtained for the Kilauea Point sequence (**Figure 10**). Firstly, the model does not predict uplift during the early onset of rejuvenated volcanism on Kaua'i. This volcanism precedes the predicted model onset by at least ~0.7 Myrs, as exemplified by the Mōkōlea Point lava event on **Figure 10**. Secondly, observed magma production rates (24 km<sup>3</sup>/Myrs; Garcia et al., 2010) are almost a factor two higher than predicted by the flexural decompression model (13 km<sup>3</sup>/Myrs; Bianco et al., 2005). Thirdly, data presented here do not match well with the model predicted rate of flexural uplift induced by loading of the Maui Nui complex (weighted loading center = West Maui) onto a Pacific plate with effective elastic plate thickness (Te) of 25 and 35 km, respectively (**Figure 10a**). However, if the weighted loading center is shifted east toward Haleakalā, then the model predicted rate of flexural uplift for the case of Te = 25 km exhibits a good match to observations of the last 1.5 Myrs, especially the peak in magma production centered on ~1.3 Ma (**Figure 10**). This is also consistent with the prediction that flexure-driven asthenosphere decompression, as Kaua'i passed over the Arch,

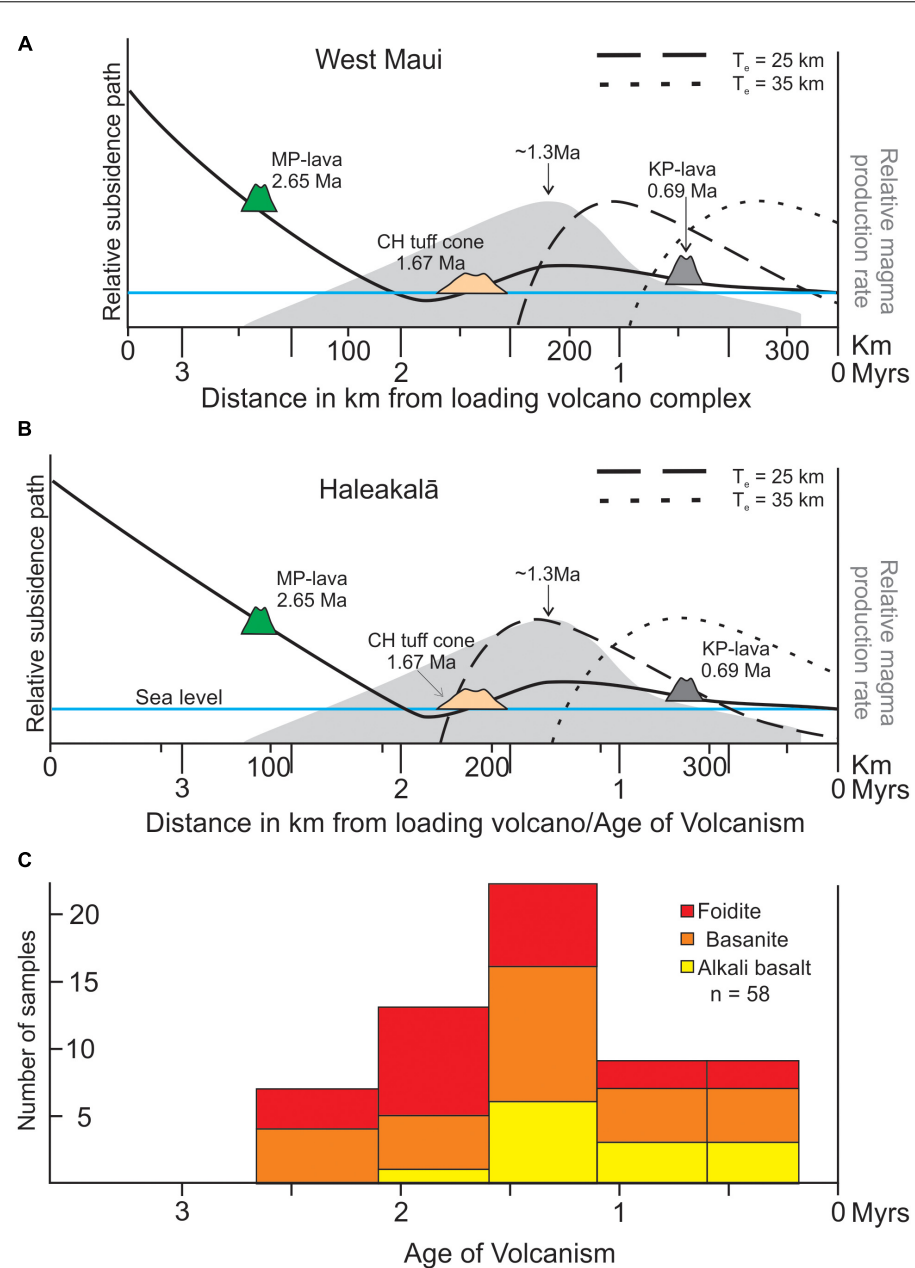


**FIGURE 10 |** Schematic representation of the subsidence history as depicted by the volcanic succession at Kilauea Point, with the weighted center of the load focus as **(A)** West Maui and **(B)** Haleakalā. Solid black curve represents the reconstructed subsidence path of the Kilauea Point area striding across the flexural arch between  $\sim 3.9$  and  $\sim 0.7$  Ma. The elevations of the Mōkōlea Point (MP) and Kīlauea Point (KP) lavas is inferred to be 500 and  $\leq 60$  m, respectively (see text for details). Temporal variation in predicted rate of flexural uplift (= magma flux rate) from the loading of the Pacific plate by Maui Nui volcanism (Bianco et al., 2005) is illustrated with broken lines for effective elastic plate thickness ( $T_e$ ) of 25 and 35 km, respectively (see key). The y-axis on the right indicates also the relative observed magma production rate (gray shaded area) as constructed by Garcia et al. (2010). The Pacific plate is assumed to have moved WNW at a rate of  $\sim 100$  km/Myr. It is noteworthy that rejuvenated volcanism began, at least,  $\sim 0.7$  Myr ( $T_e = 25$  km; Haleakalā) to about 1.8 Myrs ( $T_e = 35$  km; West Maui) earlier than predicted by the model. The observations on magmatism in the last 1.5 Ma only exhibits a reasonable fit with the model prediction for an effective elastic plate thickness  $T_e = 25$  km and Haleakalā volcano as the weighted loading center. **(C)** Histogram of rock types vs. age in  $\sim 0.5$  million-year bins. Oldest rocks are strongly alkalic, foidites and basanites and no alkali basalts. At the peak in rejuvenated volcanism on Kaua'i about 1.3 Ma, the rejuvenated magmatism is producing all three rock types and maintains that feature thereafter. Drafted based on information from Bianco et al. (2005) and Garcia et al. (2010).

increases degree of melting and magma production (Bianco et al., 2005). The change from foidite/basanite dominated magmatism to production of significant amounts of alkali basalt magma

at  $\sim 1.3$  Ma adds credence to this perception. Even so, the observations demonstrate that the flexural decompression model does not on its own capture all aspects of the rejuvenated

magmatism on Kaua‘i. The inconsistencies listed above indicate that flexural uplift (e.g., Bianco et al., 2005) or buoyancy-driven melting (Ribe and Christensen, 1999) do not fully explain the onset of rejuvenated magmatism (e.g., Garcia et al., 2010; Cousens and Clague, 2015). However, as suggested by Garcia et al. (2010), it may be possible to overcome these discrepancies by combining these two plume source models. In this context, it is noteworthy that the aerial extent of Maui Nui is estimated to have been 40% larger than that of the Big Island of Hawaii, while its mass is estimated to be 14% less (Robinson and Eakins, 2006). Also, the mass distribution is different between the two, where the main mass loading on the Big Island (i.e., Mauna Loa and Mauna Kea) is close to the islands center, but on Maui Nui it is situated at the far east end the center island (i.e., Haleakalā). Is it possible that these differences in aerial extent and mass distribution played a role in generating the observed pattern of age, rock type and geochemistry that typifies the rejuvenated magmatism on Kaua‘i.

## CONCLUSION

In general, the observations and data presented here do not provide support for the flexural decompression model of by Bianco et al. (2005) as the sole driver for rejuvenated volcanism on Kaua‘i, especially during the early stages of volcanism (2.6–2.0 Ma; **Figure 10**). However, as current models can only explain part of the key features of rejuvenated volcanism on Kaua‘i and other Hawaiian islands (see Garcia et al., 2010 for further discussion), the quest for the all-inclusive model is still on. In this context, it might be fruitful to look at the possible role of the loading-island-mass as a variable.

## REFERENCES

- Bianco, T. A., Ito, G., Becker, J. M., and Garcia, M. O. (2005). Secondary Hawaiian volcanism formed by flexural arch decompression. *Geochem. Geophys. Geosyst.* 6:Q80009, doi: 10.1029/2005GC000945
- Clague, D. A., and Frey, F. A. (1982). Petrology and trace element geochemistry of the Honolulu volcanics, Oahu: implications for the oceanic mantle below Hawaii. *J. Petrol.* 23, 447–504. doi: 10.1093/petrology/23.3.447
- Clague, D. A., Holcomb, R. T., Sinton, J. M., Detrick, R. S., and Torresan, M. E. (1990). Pliocene and Pleistocene alkalic flood basalts on the seafloor north of the Hawaiian islands. *Earth Planet Sci. Lett.* 98, 175–191. doi: 10.1016/0012-821X(90)90058-6
- Cousens, B. L., and Clague, D. A. (2015). Shield to rejuvenated stage volcanism on Kauai and Niihau, Hawaiian Islands. *J. Petrol.* 56, 1547–1584. doi: 10.1093/petrology/egv045
- Fekiacova, Z., Abouchami, W., Galer, S. J. G., Garcia, M. O., and Hofmann, A. W. (2007). Temporal evolution of Ko‘olau volcano: inferences from isotope results on the Ko‘olau scientific drilling project (KSDP) and Honolulu volcanics. *Earth Planet. Sci. Lett.* 261, 65–83. doi: 10.1016/j.epsl.2007.06.005
- Flinders, A., Ito, I., and Garcia, M. O. (2010). Gravity anomalies of the Northern Hawaiian Islands: implications on the shield evolution of Kauai and Niihau. *J. Geophys. Res.* 115:B08412. doi: 10.1029/2009JB006877
- Garcia, M. O., Grooms, D., and Naughton, J. (1987). Petrology and geochronology of volcanic rocks from seamounts along and near the Hawaiian Ridge. *Lithos* 20, 323–336. doi: 10.1016/S0024-4937(87)80005-1
- Garcia, M. O., Swinnard, L., Weis, D., Greene, A. R., Tagami, T., Sano, H., and Gandy, C. E. (2010). Petrology, geochemistry and geochronology of Kauai lavas over 4.5 Myr: implications for the origin of rejuvenated volcanism and the evolution of the Hawaiian plume. *J. Petrol.* 51, 1507–1540. doi: 10.1093/petrology/egq027
- Gurriet, P. (1987). A thermal model for the origin of post-erosional alkalic lava, Hawaii. *Earth Planet. Sci. Lett.* 82, 153–158. doi: 10.1016/0012-821X(87)90115-4
- Hansen, J., Sato, M., Russell, G., and Kharecha, P. (2013). Climate sensitivity, sea level and atmospheric carbon dioxide. *Philos. Trans. R. Soc. A* 371:20120294. doi: 10.1098/rsta.2012.0294
- Hearty, P. J. (2002). The Ka‘ena highstand of O‘ahu, Hawai‘i: further evidence of Antarctic ice collapse during the middle pleistocene. *Pac. Sci.* 56, 65–81. doi: 10.1353/psc.2002.0004
- Hearty, P. J., Karner, D. B., Renne, P. R., Olson, S. L., and Fletcher, S. (2005). 40Ar/39Ar age of a young rejuvenation basalt flow: implications for the duration of volcanism and the timing of carbonate platform development during the quaternary on Kaua‘i, Hawaiian Islands. *N. Z. J. Geol. Geophys.* 48, 199–211. doi: 10.1080/00288306.2005.9515110
- Jackson, E. D., and Wright, T. L. (1970). Xenoliths in the Honolulu volcanic series, Hawaii. *J. Petrol.* 11, 405–430. doi: 10.1093/petrology/11.2.405
- Lassiter, J. C., Hauri, E. H., Reiners, P. W., and Garcia, M. O. (2000). Generation of Hawaiian post-erosional lavas by melting of mixed lherzolite/pyroxenite source. *Earth Planet. Sci. Lett.* 178, 269–284. doi: 10.1016/S0012-821X(00)0084-4
- Lipman, P. W., Clague, A., Moore, J. G., and Holcomb R. T. (1989). South Arch volcanic field—Newly identified young lava flows on the sea floor south of the Hawaiian Ridge. *Geology* 17, 611–614. doi: 10.1130/0091-7613(1989)017<611:SAVFNI>2.3.CO;2
- Ludwig, K. R., Szabo, B. L., Moore, J. G., and Simmons, K. R. (1991). Crustal subsidence rate off Hawaii determined from 234U/238U ages of drowned coral

The following deductions on the volcanism at Kilauea Point may also be of interest. The eruptions that formed the Crater Hill tuff cone and Kilauea Point lava appear to have had conduits that followed effectively the same lineament toward the surface, despite having taken place about 1 Myrs apart. This strongly suggests that the magma that fed these eruptions, and possibly the Mōkōlea Point lava eruption as well, followed the same, preexisting structural weakness to reach the surface as implied by Macdonald et al. (1960), rather than creating their own pathway. Hence, it may be practical to explore other rejuvenated volcanic vent constructs on Kaua‘i and other islands, such as O‘ahu, in this context and assess if they exhibit similar relationships with preexisting structural lineaments. Such knowledge would be of value for volcanic risk assessment and mitigation plans regarding future rejuvenation stage eruptions on the Hawaiian Islands.

## AUTHOR CONTRIBUTIONS

TT and MG contributed equally to all aspects of the research and manuscript preparation.

## ACKNOWLEDGMENTS

We thank the Kilauea Point Wildlife Refuge, Kaua‘i for access to their land and financial support for this project. We also thank Darcy Wanless for assistance with field work, the reviewers JS and J-FW for constructive and helpful reviews. The editor RB for handling of the manuscript and chief editor Valerio Acocella for suggestions to improve the text.

- reefs. *Geology* 19, 171–174. doi: 10.1130/0091-7613(1991)019<0171:CSROHD>2.3.CO;2
- Maalo, S., James, D., Smedley, P., Petersen, S., and Garmann, L. B. (1992). The Kōloa volcanics suite of Kaua'i, Hawaii. *J. Petrol.* 33, 761–784. doi: 10.1093/petrology/33.4.761
- Macdonald, G. A., Abbott, A. T., and Peterson, F. L. (1983). *Volcanoes in the Sea: The Geology of Hawaii*. Honolulu: University of Hawaii Press.
- Macdonald, G. A., Davis, D. A., and Cox, D. C. (1960). Geology and groundwater resources of the Island of Kauai, Hawaii. *Hawaii Div. Hydrogr. Bull.* 13:212.
- Macdonald, G. A., and Katsura, T. (1964). Chemical composition of the Hawaiian lavas. *J. Petrol.* 5, 82–133. doi: 10.1093/petrology/5.1.82
- McMurtry, G. M., Campbell, J. F., Fryer, G. J., and Fietzke, J. (2010). Uplift of O'ahu, Hawaii, during the past 500 k.y. as recorded by elevated reef deposits. *Geology* 38, 27–30. doi: 10.1130/G30378.1
- Moore, J. G. (1987). "Subsidence of the Hawaiian ridge," in *Volcanism in Hawaii: U.S. Geological Survey Professional Paper 1350*, Vol. 1, eds R. W. Decker, T. L. Wright, and P. H. Stauffer, 85–100. Available at: <https://pubs.usgs.gov/pp/1987/1350/>
- Ribe, N. M., and Christensen, U. R. (1999). The dynamical origin of Hawaiian volcanism. *Earth Planet. Sci. Lett.* 171, 517–531. doi: 10.1016/S0012-821X(99)00179-X
- Robinson, J. E., and Eakins, B. W. (2006). Calculated volumes of individual shield volcanoes at the young end of the Hawaiian ridge. *J. Volcanol. Geothermal Res.* 151, 309–317. doi: 10.1016/j.jvolgeores.2005.07.033
- Self, S., Keszthelyi, L., and Thordarson, T. (1998). The importance of pahoehoe. *Annu. Rev. Earth Planet. Sci.* 26, 81–110. doi: 10.1146/annurev.earth.26.1.81
- Sherrod, D. R., Izuka, S. K., and Cousens, B. (2015). "Onset of rejuvenated-stage volcanism and the formation of lihue basin: Kaua'i events that occurred 3–4 million years ago" in *Hawaiian volcanoes: from Source to Surface. American Geophysical Union Monograph*, Vol. 208. eds R. Carey, V. Cayol, M. Poland, and D. Weis, 105–124.
- Sherrod, D. R., Sinton, J. M., Watkins, S. E., and Brunt, K. M. (2007). *Geologic Map of the State of Hawaii*. US Geological Survey Open-File Report, 2007–1089. Available at: <https://pubs.usgs.gov/of/2007/1089/>
- Sinton, J. M., Eason, D. E., and Duncan, R. A. (2017). Volcanic evolution of Moloka'i, Hawai'i: implications for the shield to postshield transition in Hawaiian volcanoes. *J. Volcanol. Geothermal Res.* doi: 10.1016/j.jvolgeores.2017.04.011
- Thorarinsson, S. (1967). *Surtsey - The New Island in the North Atlantic*. New York, NY: Viking Press, 105.
- Thordarson, T., and Self, S. (1998). The Roza Member, Columbia River Basalt Group – a gigantic pahoehoe lava flow field formed by endogenous processes. *J. Geophys. Res.* 103, 27411–27445. doi: 10.1029/98JB01355
- Walker, G. P. L. (1990). Geology and volcanology of the Hawaiian islands. *Pac. Sci.* 44, 315–347.
- Wessel, P. (1993). A reexamination of the flexural deformation beneath the Hawaiian Islands. *J. Geophys. Res.* 98, 12177–12190. doi: 10.1029/93JB00523
- Wilmoth, R. A., and Walker, G. P. L. (1993). P-type and S-type pahoehoe: a study of vesicle distribution patterns in Hawaiian lava flows. *J. Volcanol. Geothermal Res.* 55, 129–142. doi: 10.1016/0377-0273(93)90094-8
- Yamasaki, S., Sawada, R., Ozawa, A., Tagami, T., Watanabe, Y., and Takahashi, E. (2011). Unspiked K-Ar dating of Koolau lavas, Hawaii: evaluation of the influence of weathering/alteration on age determinations. *Chem. Geol.* 287, 41–53. doi: 10.1016/j.chemgeo.2011.05.003
- Yang, H. J., Frey, F. A., and Clague, D. A. (2003). Constraints on the source components of lavas forming the Hawaiian North Arch and Honolulu Volcanics. *J. Petrol.* 44, 603–627. doi: 10.1093/petrology/44.4.603

**Conflict of Interest Statement:** The authors declare that the research was conducted in the absence of any commercial or financial relationships that could be construed as a potential conflict of interest.

Copyright © 2018 Thordarson and Garcia. This is an open-access article distributed under the terms of the Creative Commons Attribution License (CC BY). The use, distribution or reproduction in other forums is permitted, provided the original author(s) and the copyright owner(s) are credited and that the original publication in this journal is cited, in accordance with accepted academic practice. No use, distribution or reproduction is permitted which does not comply with these terms.